JOURNAL OF Applied Polymer SCIENCE

Synthesis of Highly Loaded and Well-Controlled Magnetic Beads via Emulsion Polymerization

Sergei Kniajanski, Robert E. Colborn, Brian C. Bales, Orrie Riccobono, Aaron J. Dulgar-Tulloch, Judith Stein, Binil I. I. Kandapallil

General Electric Global Research Center, 1 Research Circle, Niskayuna, NY 12309

Correspondence to: B. I. I. Kandapallil (E-mail: kandapal@ge.com)

ABSTRACT: Superparamagnetic iron oxide (SPIO) incorporated polystyrene beads of uniform size distribution (~170 nm) and high magnetic content (~40%) are synthesized by emulsion styrene polymerization in the presence of functionalized SPIO. The role of surface functionality on the polymerization process and SPIO incorporation is investigated by carrying out styrene emulsion polymerizations with different functionalities on SPIO. A unique combination of oleic acid and (2-acetoacetoxy) ethyl methacrylate as surface ligands for SPIO is used to attain the best magnetic beads. © 2012 Wiley Periodicals, Inc. J. Appl. Polym. Sci. 000: 000–000, 2012

KEYWORDS: superparamagnetic iron oxide; magnetic beads; emulsion; polystyrene

Received 6 July 2012; accepted 13 November 2012; published online

DOI: 10.1002/app.38857

INTRODUCTION

Nanotechnology has made a profound impact on different aspects of medicine and has the potential to bring a paradigm shift to existing biomedical technologies. Magnetic beads have become important tools for a number of applications including purification of proteins, separation of virus, genomic sequencing, and so on.[1–3] A number of magnetic bead based devices for biochemical detection, cell-sorting, and flow-cytometry are being developed.[4] Another emerging technology is the free-flow magnetophoresis which is a method of separating magnetic particles in a continuous flow through a field flow fractionation, where magnetic particles entrained in laminar flow experience a perpendicular force due to an applied magnetic gradient and are transitioned to neighboring collection streams. The distance which each magnetic particle travels can be controlled by varying the magnetic properties of the bead, the magnetic gradient across the chamber, and the length of time the magnetic particle experiences the gradient.[5] For magnetic separation based applications to be successful, magnetic beads must be developed that offer precise control over size and magnetic content. There have been significant efforts on the synthesis of superparamagnetic iron oxide (SPIO) nanoparticles (NPs) of well-defined size as well as relentless attempts to incorporate them into magnetic beads.[6–22]

The goal of making well-controlled magnetic beads with tunable magnetic properties can be approached in various ways. Inorganic matrices (such as silica)[6] or organic matrices [such as polystyrene (PS)] have been extensively used for this purpose. Although silica scaffold is characterized by better chemical stability, lower toxicity, and higher versatility for surface modification reactions, polymer matrices seem to be more preferable from the point of view of their lower density and thus a slower gravitational sedimentation rate. As to PS beads, a variety of polymerization methods have been used including emulsion polymerization,[7] dispersion polymerization,[16–18] and more extensively miniemulsion polymerization.[19–22] As pointed out by Lansalot[20] and coworkers, most approaches fail due to one or more of the following issues: (i) inhomogeneous distribution of the NPs in the bead population, (ii) large particle size and bead size distributions, and (iii) limited loading of magnetic NPs.

Styrene emulsion polymerization without addition of fillers such as SPIO has been refined[23] and offers the advantage of a low-density matrix. This feature minimizes sedimentation during separation and offers precise size control, both of which are critical for generation of a uniform bead population. In addition, this approach offers alternatives to the heavily exploited preparation of SPIO-impregnated magnetic beads,[24] which can be easily performed but does not offer the uniform distribution of magnetic material necessary for free-flow magnetophoresis.

Herein, we describe our efforts to incorporate SPIO particles containing different surface functionalities (single and mixed) into PS beads. In our approach, SPIO NPs with customized surface properties were synthesized by different approaches followed by carrying out emulsion polymerization to obtain

© 2012 Wiley Periodicals, Inc.

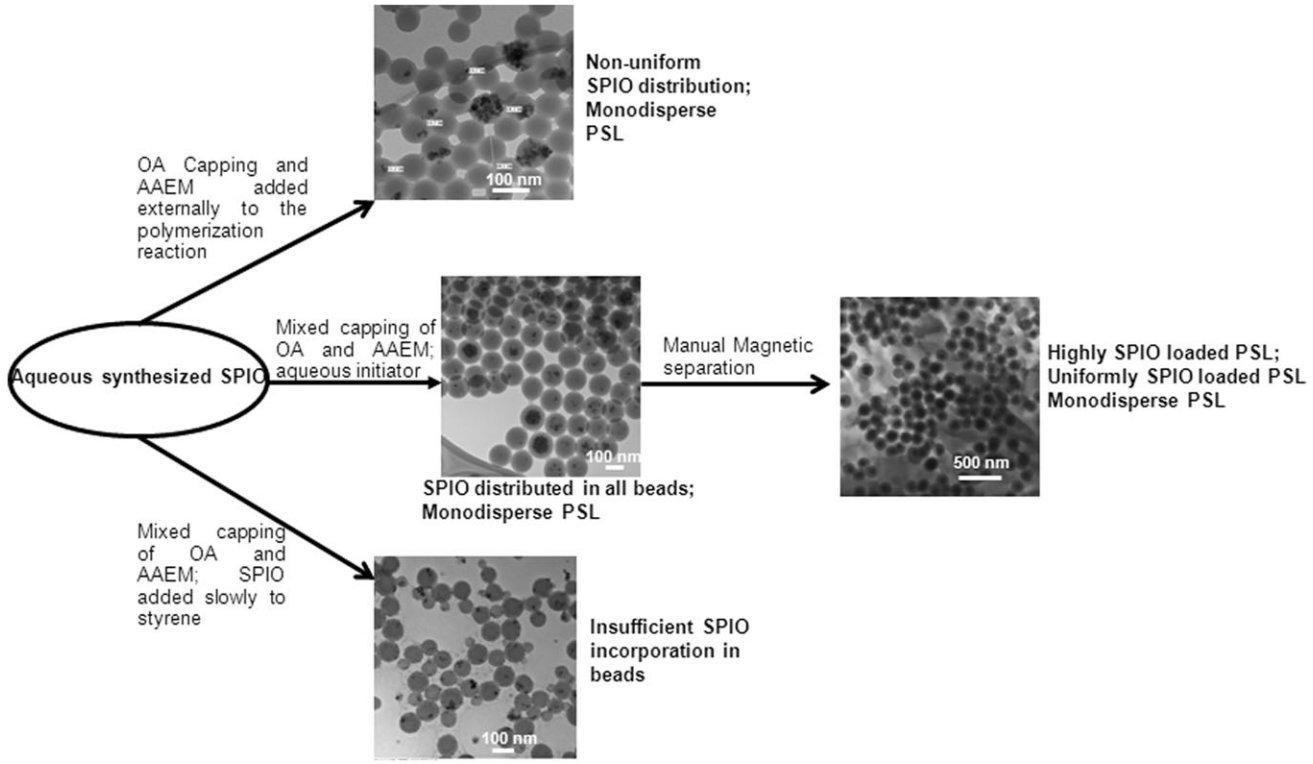

Scheme 1. Different strategies adapted for attaining magnetic beads.

magnetic beads. A schematic outline of the whole process is represented in Scheme 1. PS-SPIO emulsions having narrow bead size distribution and high SPIO loading were obtained using SPIO particles containing mixed ligands of OA and (2-acetoacetoxy) ethyl methacrylate (AAEM), in the styrene emulsion polymerization.[20]

EXPERIMENTAL SECTION

Materials and Methods

Deionized water (18.2 Mohm) was used in all experiments. The following materials were used as received: oleic acid (OA), OA sodium salt, sodium persulfate (SPS), lauroyl peroxide, diazacyanovaleric acid, styrenesulfonic acid (SSA), sodium dodecylphenylsulfonate, sodium dodecylsulfonate (SDS), citric acid (CA), AAEM, ferric chloride, ferrous chloride (all from Aldrich). Styrene (Aldrich) was stirred with aluminum oxide for 12 h, filtered through a glass filter, and vapor-recondensed in vacuum at 30–35°C. Purified styrene was stored under –5°C. Hydrodynamic particle size distributions were obtained by dynamic light scattering (DLS) technique using Brookhaven ZetaPals Analyzer fitted with a 90Plus particle analyzer. Transmission electron microscopy (TEM) images were obtained using a FEI CM 100 electron microscope operated at 100 kV. Samples were prepared by drying dilute solutions on a carbon grid.

SPIO Syntheses

Aqueous SPIO-OA. A solution of $FeCl_36H_2O$ (16 mmol) and $FeCl_24H_2O$ (8 mmol) in 100 mL water was stirred under N_2 for 15 min. To this mixture, 11.6 mL of NH_4OH (28%) was added dropwise, and the resulting solution was stirred for 1 h. The iron oxide particles formed were washed by repeated magnetic decantation with deionized water until the solution has become neutral. When OA is added at neutral pH, the iron oxide particles are suspended in approximately 90 mL water followed by addition of specific amounts of sodium oleate. When the ligand addition is carried out at pH 4, the iron oxide is resuspended in ~90 mL of 0.01 M HCl followed by addition of 1 mL 0.1 M HCl. After addition of the ligand, the reaction mixture is stirred at 95°C for 1 h using a mechanical stirrer and the resulting SPIO solution is further bath-sonicated for 20 min to get the final NP solution.

Aqueous SPIO-SDS. A solution of $FeCl_3.6H_2O$ (4 mmol) and $FeCl_2.4H_2O$ (2 mmol) in 100 mL water was stirred under N_2 for 15 min. A SDS solution, prepared by dissolving 200 mg in 200 mL of water, was added dropwise to this solution so that Fe/SDS ratio was 10. After stirring the resulting mixture for 30 min, NH_4OH (3 mL) was added and stirred further for 1 h. The NP suspension was purified by magnetic decantation and further bath-sonication for 40 min after resuspending in ~100 mL water.

Aqueous SPIO-CA. A mixture of $FeCl_3.6H_2O$ (4 mmol) and $FeCl_2.4H_2O$ (2 mmol) was dissolved in 25 mL water. After stirring under N_2 for 15 min, 2.5 mL NH_4OH was added slowly and the reaction mixture was stirred for 30 min. After magnetic decantation and washing with water until pH was 7–8, sodium citrate (720 mg, 0.6 mmol) in 5 mL water was added, followed by 25 mL water. After sonicating in a bath for 20 min, the solution was stirred at 95°C overnight. The NPs were centrifuged

and the supernantant, which was filterable through 0.2-μ filter, was used for polymerization reactions.

Aqueous SPIO Synthesis using Gallic Acid. The synthesis was done exactly as described for SPIO-CA. In a typical preparation, $FeCl_3.6H_2O$ (4 mmol) and $FeCl_2.4H_2O$ (2 mmol) was reduced with NH_4OH (2.5 mL), washed multiple times using magnetic decantation, and treated with gallic acid (102 mg). After sonication and stirring at 90°C for 8 h, the NPs could be filtered through a 0.2-μ filter.

Aqueous SPIO-SSA. The synthetic strategy was similar to that of OA-capped NPs. However, in both cases of PS sulfonate and styrene sulfonate (SS), the final NP solution was less stable and precipitated over time.

Aqueous SPIO-OA-AAEM and SPIO-OA-SSA. Synthesis of SPIO with mixed ligands was carried out similar to that of OA-capped NPs. In the ligand addition step, OA was added first followed by the second ligand (AAEM or SSA) in appropriate molar equivalents.

Styrene Emulsion Polymerization in the Presence of Water Soluble SPIO

Polymerizations were performed in 300 mL three-neck round bottom flasks equipped with nitrogen inlet, mechanic stirrer, thermometer, and a condenser capped with a nitrogen outlet. The flask was charged with 100 mL of deionized water containing necessary amount of SPIO (1–40 wt % relative to styrene). Optionally, 0.166–0.333 g of AAEM (2.5-5 wt% to styrene) was added. The mixture was stirred under fast nitrogen flow for 1 h. Styrene (6.65 g) was added through thermometer inlet. The nitrogen flow was reduced to 1–2 mL/s, and the system was purged for 30 min with stirring speed set up to 350–550 rpm using a stroboscope. A solution of 0.15 g of a water soluble initiator (SPS or diazacyanovaleric acid) in 2 mL of deionized water was added, and the mixture was heated to 65–67°C. Polymerization time was 7–12 h. The polymerizations were quenched by cooling the reaction flask and introducing air.

Styrene conversion was determined by drying PS/SPIO sediments (separated from the liquid phase by centrifugation) in vacuum at 50°C overnight. The weights of dried materials from 12-h polymerization reactions did not differ more than 3–5% from the total reaction charge (SPIO + OA + AAEM + styrene), indicating almost absolute yield for the reaction.

RESULTS AND DISCUSSION

SPIO Syntheses

We focused our efforts on water-born SPIO because this method produces larger particles with higher magnetization. To achieve the set goals, we have tuned the physicochemical properties of SPIO by synthesizing them under different conditions (including different ligands, multiple ligands, pH, ligand ratio to Fe, and so on) which will be summarized in this section. Details on the synthesis of SPIO particles are in the experimental section. The details on our efforts to incorporate these SPIO NPs into PS beads are explained in the next section.

It is imperative to prepare SPIO with uniform size distribution, possessing uniform and well-defined magnetic properties so that beads of specific magnetic moments can be synthesized. The synthesis of SPIO NPs coated with several different stabilizers was carried out to evaluate the effect of the surface stabilizer on the ability to incorporate the SPIO NPs into a PS matrix in a well-defined manner. The most popular and successful synthesis of aqueous SPIO utilizes OA as a stabilizing ligand.[5] It is believed that water solubilization of SPIO using OA results from bilayer formation of the ligands where the carboxylic acid groups in the first layer anchor on the NP surface while the carboxylic groups on the second layer protrude outward, imparting hydrophilicity.[24,25] Therefore, varying the concentration of OA during SPIO synthesis is expected to influence NP solvophobicity, which in turn could impact the SPIO incorporation into the styrene matrix. We carried out a limited number of syntheses by varying the OA concentration with respect to iron and also by changing the pH of the reaction, which resulted in significantly different sized NPs. Two approaches were used for changing pH of reactions: (1) sodium oleate was added after adjusting the pH of the iron oxide suspension to 4 using 0.1 M HCl; (2) sodium oleate was added to a neutral solution of the NPs. The properties of different NPs were obviously different and are summarized in Table I (runs 1–4).

Table I. Properties of SPIO Particles

Run	Ligand	Ligand/Fe	pH at ligand addition	Size (DLS), nm
1	OA	2/3	7	35 (75%), 180 (25%)
2	OA	1/3	7	80
3	OA	1/3	4	30
4	OA	1/6	4	250
5	SDPS	1/75	4	200
6	SDPS	1/10	4	35
7	Sodium Citrate	1/10	4	35
8	Gallic acid	1/10	4	30

In addition to OA being used under different conditions for tuning the SPIO properties, ligands having functional/chemical similarity with styrene were used for SPIO synthesis to tune their solvophobicity and hence compatibility with PS beads. New ligands such as sodium dodecyl phenyl sulfate (SDPS), sodium citrate, and gallic acid were used to make SPIO NPs (Table I, runs 5–8).

SPIO NPs of sizes from 200 to 30 nm were synthesized by varying the Fe/SDPS mole ratio followed by ultrasonication of the NP suspension. CA-capped SPIO particles with an average size of 35 nm were successfully synthesized and purified by centrifugation to remove any large aggregates. Similarly, gallic acid-capped SPIO particles (30 nm size) were also synthesized. Both CA- and gallic-acid-capped SPIO particle solutions are stable at sufficiently high concentrations required for emulsion polymerization and could easily be filtered through 0.2-μ filters. NPs were also synthesized using poly(sodium-4-styrene)sulfonate[26] as well as the corresponding monomer, styrene-4-sodiumsulfonate. In both

Table II. Properties of SPIO with Mixed Ligands

Run	Coligand	OA (mole ratio to Fe)	Coligand (mole ratio to Fe)	Size (DLS), nm
9	AAEM	1/6	1/3	50
10	AAEM	1/12	1/3	Aggregated
11	AAEM	1/8	1/3	80–90
12	AAEM	1/6	1/5	70
13	AAEM	1/5	1/3	35
14	SS	1/6	1/6	45
15	SS	1/6	1/3	30

cases, the NPs were not completely water-soluble after capping, presumably because the hydrophilic moieties on these ligands once attached to the NP surface are no longer available to impart water solubility.

In another approach, polymerizable AAEM[20] was used as a coligand with OA during SPIO synthesis (Table II). It should also be noted that AAEM once attached to SPIO surface, could be more reactive than styrene and, hence could be prone to self-polymerization, resulting in aggregation of SPIO during PS bead synthesis. In yet another attempt to improve NP incorporation, AAEM was substituted with SS in an effort to match the reactivities between styrene in solution and polymerizable moiety on the NP surface. Different reactions attempted using OA and SS gave reasonably monodisperse SPIO particles (Table II, runs 14, 15).

Polymerization

Now that we have achieved SPIO NPs with a wide range of surface functionality and hence potentially different polymerizability with styrene, we carried out polymerization reactions under different conditions. Styrene emulsion radical polymerization can be performed either with water-soluble initiators (e.g., SPS) or styrene-soluble initiators (e.g., lauroyl peroxide). However, successful incorporation of functionalized SPIO NPs into PS beads was only achieved with water-soluble initiators. Products obtained from polymerizations using styrene soluble initiator consisted of polydisperse, small PS beads bearing aggregated SPIO on the surface.

In an attempt to reproduce reported results[20] using OA-capped SPIO, we found that our PS latex (PSL) consisted of much smaller beads (~140 nm vs. ~450 nm[20]), but with a fairly narrow bead size distribution [Figure 1(a)]. We explain this discrepancy by two reasons: (1) possibly better stirring uniformity at more appropriate Reynolds number, and (2) different amount of OA on the SPIO surface (due to ambiguity in the reference[20]).

The SPIO aggregate size and its distribution shown in Figure 1(a) roughly correspond to the DLS data obtained for the initial SPIO solution (~80 nm, entry 2 in Table II) when taking into account the tendency of DLS to overestimate the particle size due to solvation effects.

It is notable here that more than half of the PS beads do not contain SPIO, which can be probably explained by the low SPIO concentration in the polymerization reaction. Also, the loaded beads contain only one SPIO particle as either a primary particle or an aggregate. Another peculiarity of this sample consists in fairly narrow bead size distribution wherein both empty and loaded PS beads have similar sizes. These results can be explained in terms of the presence of large amount of organic ligands in the polymerization reaction, on emulsifying styrene in water in the presence of SPIO, the outer OA layer of the double layer, which imparted hydrophilicity to the SPIO, is no longer needed to stabilize the SPIO in styrene misceles. A single layer of OA is now sufficient to provide SPIO compatibility with styrene. In addition, some of the OA molecules are replaced with AAEM. Thus, the released OA and probably, excess of OA in the initial SPIO suspension, acts as a surfactant in the emulsion. Thus, after 30 min of stirring OA is evenly distributed in the emulsion providing uniform size for all miscells independent of the SPIO loading. These emulsions, however, are not stable and segregate into colorless aqueous and brown organic layers within 20 min once stirring is stopped. Complete transfer of SPIO into styrene also suggests the conversion of OA double layer on SPIO into a monolayer thus imparting SPIO compatibility with the organic phase.

In contrast to the reaction with 0.83 wt % SPIO added, polymerization with 4.2 wt % SPIO (from Run 3 Table I) and 5% AAEM yielded ~70 nm PSL beads under similar polymerization conditions [Figure 1(b)]. Note that AAEM was added into the polymerization reaction in these cases. The formation of smaller sized PSL results from the increased amount of SPIO in the reaction, which in turn leads to an addition of five times more OA in the polymerization system. The OA works as a surfactant and decreases the PS bead size. Other differences are: fewer SPIO loaded beads and the presence of larger SPIO aggregates. The number of primary SPIO particles seems to decrease with increased SPIO concentration, which can be interpreted as an enhanced tendency of SPIO to aggregate at higher concentrations.

Different approaches were used to keep SPIO from aggregating during the polymerization. Increased amount of OA (2/3 equivalent to total iron) in the SPIO synthesis gave a SPIO solution containing mostly primary 12–15 nm iron oxide particles. However, the use of this solution in the emulsion polymerization resulted in PSL with a bead size around 50 nm, which is consistent with the effect of increased amount of OA in the polymerization. In another approach, the aqueous SPIO was successfully transferred into styrene by magnetically separating the SPIO/OA from the aqueous solution, rinsing it with DI water, and finally dispersing in styrene. This procedure yielded a solution containing mostly primary SPIO particles. Nevertheless, polymerization with this product resulted in SPIO separation from off-white PSL, potentially because of reduced amount of OA on the NPs after the aforementioned magnetic separation step.

Given the observed PS bead size, it appears that the styrene polymerization in the presence of OA-capped SPIO occurs in the microemulsion regime as a result of the high surfactant level

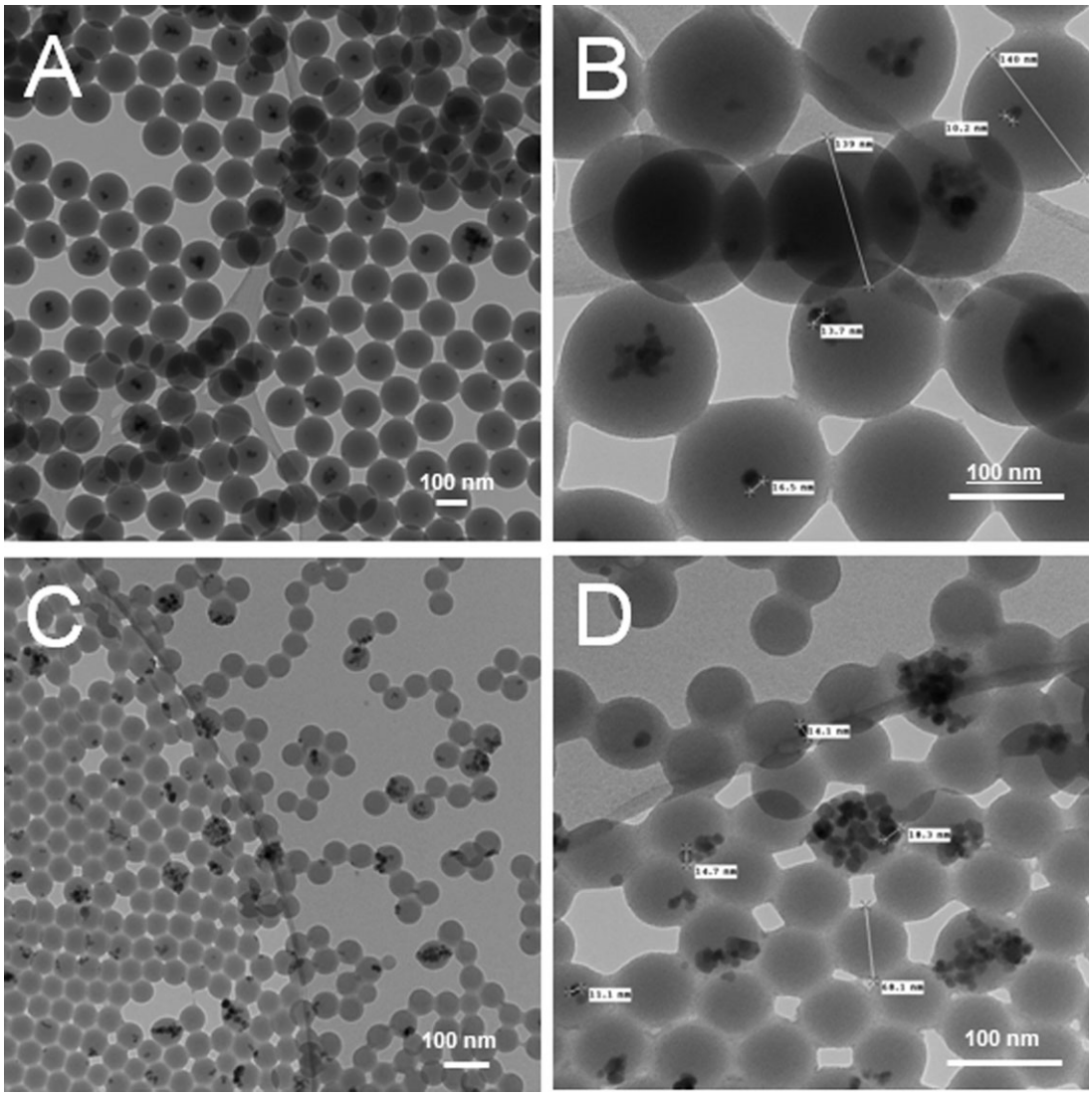

Figure 1. TEM images of PSL obtained with 0.83 wt % of Fe3O4-1/3OA and 5% AAEM (A, B), and 4.2 wt % of Fe3O4-1/3OA and 5% AAEM (C, D).

of the SPIO-OA solution. Our attempts to shift the polymerization toward larger bead sizes were unsuccessful. Changing the stirring rate (Reynolds number), amount of AAEM added to the polymerization reaction, amount of styrene, and the initiator concentration either did not change the bead size or resulted in the formation of large aggregates of 50–60 nm primary PS beads. The effect of SPIO-OA can be clearly elucidated by comparing the above results to the PS beads of 280–300 nm (by DLS) obtained under similar polymerization conditions in the absence of SPIO-OA.

Styrene emulsion polymerization performed with an aqueous solution of SPIO-SDS (sodium dodecylsulfate) resulted in the separation of SPIO from the latex and formation of a SPIO-containing solid phase. SDPS-functionalized NPs were not stable at concentrations high enough to achieve significant (>3%) SPIO incorporation into PS beads on emulsion polymerization of styrene. SPIO coated with CA was not incorporated into PS beads even though SPIO did not separate from the PSL solution. The PS bead size was 350–460 nm, which indicates that citrate does not act as a surfactant. Thus, the key to increasing the PS bead size is the reduction of OA concentration while keeping the SPIO particles from agglomeration by adding a nonsurfactant which could also serve as coligand. AAEM was found to be a good candidate for this approach.

A number of SPIO's containing different loadings of OA and AAEM were synthesized and the screening matrix of the coating composition is shown in Table III along with the polymerization results. The ligand amounts (OA and AAEM) are represented as molar equivalents to total iron. The polymerization

Table III. SPIO Coating Composition and Resulting PS Beads Size in nm

OA AAEM	1/5	1/6	1/8
2/5		60	
1/3	155 broad	250-265	200
1/5		90	

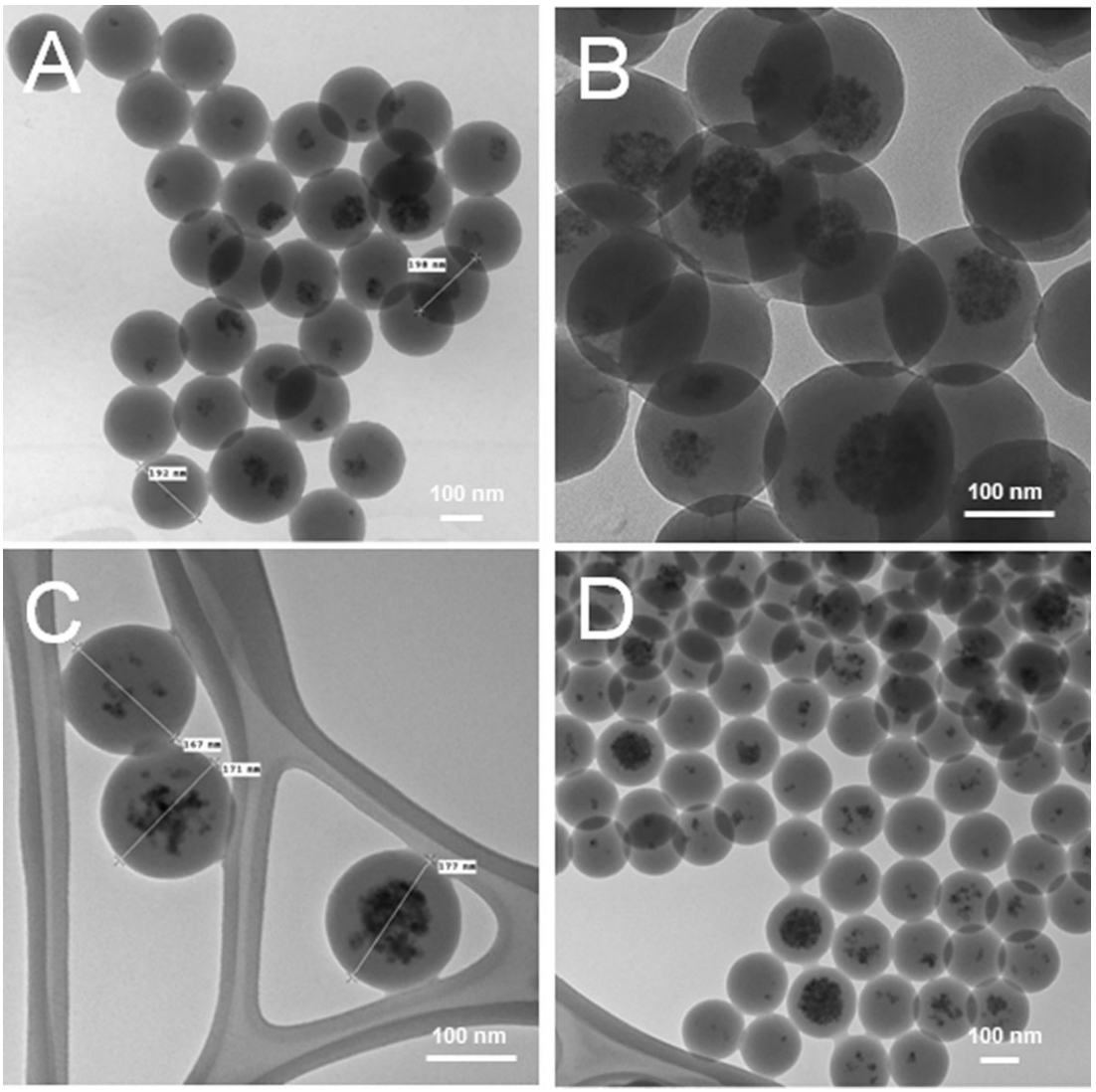

Figure 2. TEM images of PSL with SPIO-1/6OA-1/3AAEM (14.6 wt % Fe) at different magnifications (A, B), and SPIO-1/8OA-1/3AAEM (15.0 wt % Fe) (C, D).

results are bead diameters in nm as determined by DLS. The polymerizations were performed with 12–20 wt % iron loadings. High SPIO amounts were used to facilitate the formation of the maximum population of PS beads loaded with SPIO. Surprisingly, the bead diameter has a strong, nonlinear dependence on the coating composition. This circumstance significantly complicates the process optimization. Nonetheless, it can be tentatively assumed that the result obtained for 1/6OA-1/3AAEM composition is close to the maximum possible bead size (~250 nm). The TEM images of the most remarkable samples are shown in Figure 2(a,b).

Using these conditions, most of the PS beads have at least one primary SPIO particle as evidenced from TEM images. However, the SPIO distribution is broad, ranging from a single particle to 100 nm aggregates. Moreover, in many cases the SPIO core is not in the center of a bead, which suggests that SPIO may have aggregated after being incorporated into the PS beads. Indeed, the images of a sample made with SPIO-1/8OA-1/3AAEM (15.0 wt % SPIO) revealed PS beads containing more than one SPIO particle (ether primary particles or aggregates) [Figure 2(c,d)]. It was hypothesized that the SPIO aggregation in the styrene emulsion polymerization resulted from homopolymerization of the acrylic moieties in the AAEM molecules. This was confirmed by running the polymerization with a significantly increased SPIO amount (~47 wt % loading). The SPIO aggregation started before the latex formation, resulting in the formation of a single black piece of aggregated SPIO, whereas the PSL contained only traces of iron oxide. One of the possible explanations for the observed phenomenon can be as follows: despite the fact that both acrylic and styrenic groups are reactive to free radical polymerization and have been successfully copolymerized in a random way in many cases,[27] their relative reactivity may change in the presence of SPIO. The electron density is shifted to the acetylacetone moiety when AAEM is coordinated to the iron oxide NP. The acrylic moiety,

therefore, becomes more reactive and more prone to homopolymerization. As a result, the formation of acrylic–acrylic sequences is favored over the formation of acrylic–styrene and styrene–acrylic sequences.

The obtained PS-SPIO latexes with 15–19 wt % (based on the amount of SPIO added and assuming 100% incorporation) iron loading can be magnetically separated into fractions containing different amounts of SPIO. The separation is based on the time necessary to move the beads of the aqueous solution in the presence of a magnetic field. This separation was carried out manually using 0.4 T permanent magnets of 1.5 inch diameter. First, a fraction was collected after a 30 s run through 1.5 cm aqueous layer and isolated from the original latex. A second fraction was then collected after a 10 min run through the 1.5 cm aqueous layer and was isolated. The first, dark-brown, fraction represents about 0.3 wt % of the total material. It consists of the heavily SPIO loaded beads that sediment very fast because of their high density and exhibit partial aggregation in dilute aqueous solution. The second, brownish fraction, represents about 1.5 wt % of the total material and does not aggregate in solution. TEM images of this solution (Figure 3) show uniform distribution of the SPIO aggregates across the PS beads. Thus, the obtained latexes can be magnetically separated by means of an available technique (either manual or automatic) to obtain monodisperse PS beads with relatively narrow SPIO distribution.

Vibrating sample magnetometer (VSM) measurements on the magnetic beads before magnetic separation [see Figure 2(a), 15.2 wt% loading by TGA] and after magnetic separation (see Figure 3, 40.1 wt % by TGA) were performed and are shown in Figure 4. As expected for superparamagnetic materials, neither coercivity nor remanence was observed in either case. The saturation magnetizations of the bulk PSL and magnetically separated fraction were 8 and 20 emu/g, respectively, which indicates that the ratio of iron content is consistent with TGA analysis. The saturation magnetization value of the synthesized SPIO was thus calculated as 52 emu/g, in agreement with the typical M_{sat} of the water-born SPIO (50–60 emu/g).[28] This indicates the very high loading of SPIO (~40%) in the PS beads has been achieved with the current strategy.

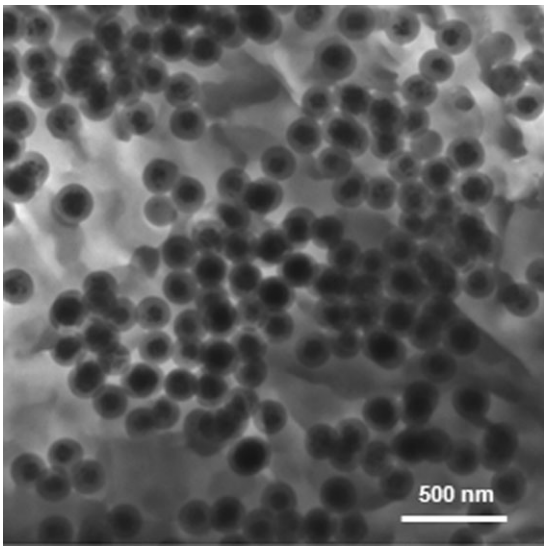

Figure 3. TEM image of a fraction magnetically separated from a PSL obtained with SPIO-OA-AAEM (14.6 wt % Fe loading).

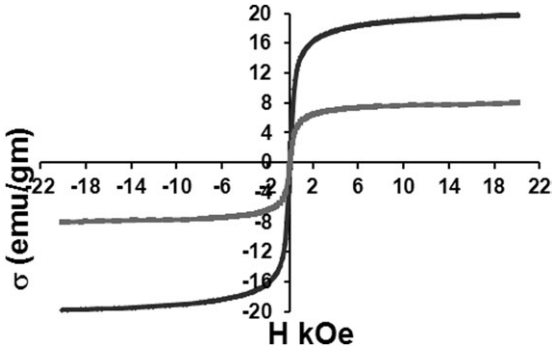

Figure 4. Room temperature VSM measurements of bulk PSL obtained with 14.6 wt % of SPIO-OA-AAEM (gray line) and its fraction magnetically separated in 10 min (black line).

CONCLUSIONS

Water-dispersible SPIO-OA-AAEM in combination with a water-soluble initiator produces monodisperse PSL with SPIO incorporated into the PS beads. However, the OA coating on the SPIO surface acts as a surfactant, and the polymerization occurs in the microemulsion regime yielding PS beads not larger than about 200 nm (TEM data; 250 nm by DLS). Tuning the polymerization conditions does not shift the reaction toward bigger PS beads. At the same time, SPIO is aggregated under the polymerization conditions due to the presence of acrylic groups on its surface. This aggregation limits the amount of iron oxide, which can be loaded to the PSL beads. At high SPIO concentrations (between 19 and 45 wt % SPIO), the homopolymerization of acrylic moieties leads to complete SPIO separation from the latex. At low to medium concentrations (<1 to 5 wt %), SPIO aggregates of different sizes are formed. Surprisingly, the PS bead size is independent of the SPIO nucleus size and is even similar to that of the beads, which do not contain any SPIO. As a result, monodisperse beads with a nonuniform SPIO distribution are obtained. We have also demonstrated the ability to fractionate a highly SPIO loaded PSL bead population (~40% loading by weight) from a reaction mixture using manual magnetic separation.

The bead size distribution of the PSL prepared is fairly narrow. This represents a significant improvement over previous studies, which usually report a broad bead size distribution. The size of the magnetic beads obtained here may not be ideal for cell separation (1 micron size is desirable for rapid isolation at moderate field strengths) but may enable separation of smaller natural objects such as DNA, proteins, and so on. The ability to magnetically separate the prepared latexes into fractions with different content of magnetic material potentially also enables multiplex separation.

REFERENCES

1. Haukanes, B. I.; Kvam, C. *Nat. Biotechnol.* **1993**, *11*, 60.
2. Rahman, M. M.; Elaissari, A. *J. Colloid Sci. Biotechnol.* **2012**, *1*, 3.
3. Arkhis, A.; Elaissari, A.; Delair, T.; Verrier, B.; Mandrand, B. *J. Biomed. Nanotechnol.* **2010**, *6*, 28.
4. Weddemann, A.; Wittbracht, F.; Auge, A.; Hütten, A. *Appl. Phys. Lett.* **2009**, *94*, 173501.
5. Tarn, M. D.; Peyman, S.A. Robert, D.; Iles, A.; Wilhelm, C.; Pamme, N. *J. Magn. Magn. Mater.* **2009**, *321*, 4115.
6. Laurent, S.; Forge, D.; Port, M.; Roch, A.; Robic, C.; Vander Elst, L.; Muller, R. N. *Chem. Rev.* **2008**, *108*, 2064.
7. Zhao, W.; Shi, J.; Chen, H.; Zhang, L. *J. Mater. Res.* **2006**, *21*, 3080.
8. Ma, D.; Veres, T.; Clime, L.; Normandin, F.; Guan, J.; Kingston, D.; Simard, B. *J. Phys. Chem. C* **2007**, *111*, 1999.
9. Insin, N.; Tracy, J. B.; Lee, H.; Zimmer, J. P.; Westervelt, R. M.; Bawendi, M. G. *ACS Nano* **2008**, *2*, 197.
10. Choi, W.-S.; Koob, H.-Y.; Huck, W.T. S. *J. Mater. Chem.* **2007**, *17*, 4943.
11. Sun, Y.; Duan, L.; Guo, Z.; DuanMu, Y.; Ma, M.; Xu, L.; Zhang, Y.; Gu, N. *J. Magn. Magn. Mater.* **2005**, *285*, 65.
12. Zhou, X.; Kobayashi, Y.; Romanyuk, V.; Ochuchic, N.; Takedac, M.; Tsunekawad, S.; Kasuya, A. *Appl. Surf. Sci.* **2005**, *242*, 281.
13. Steitz, B.; Krauss, F.; Rousseau, S.; Hofmann, H.; Petri-Fink, A. *Adv. Eng. Mater.* **2007**, *9*, 375.
14. Lou, M.-Y.; Jia, Q.-L.; Wang, De-P.; Liu, B.; Huang. W.-H. *J. Mater. Sci: Mater. Med.* **2008**, *19*, 217.
15. Montagne, F.; Mondain-Monval, O.; Pichot, C.; Elaïssari, A. *J. Polym. Sci. Part A: Polym. Chem.* **2006**, *44*, 2642.
16. Kondo, A.; Kamura, H.; Higashitani, K. *Appl. Microbiol. Biotechnol.* **1994**, *41*, 99.
17. HoraK, D.; Semenyuk, N.; Lednický, F. *J. Polym. Sci., Part A: Polym. Chem.* **2003**, *41*, 1848.
18. Niu, M.; Du, M.; Gao, Z.; Yang, C.; Lu, X.; Qiao, R.; Gao, M. *Macromol. Rapid. Commun.* **2010**, *31*, 1805.
19. Zhang, Q.; Xie, G.; Zhang, H.; Zhang, J.; He, M. *J. Appl. Polym. Sci.* **2007**, *105*, 3525.
20. Joumaa, N.; Toussay, P.; Lansalot, M.; Elaissari, A. *J. Polym. Sci., Part A: Polym. Chem.* **2008**, *46*, 327.
21. Pich, A.; Bhattacharya, S.; Ghosh, A.; Adler, H.-J. P. *Polymer* **2005**, *46*, 4596.
22. Medeiros, S. F.; Santos, A. M.; Fessi, H.; Elaissari, A. *J. Colloid Sci. Biotechnol.* **2012**, *1*, 99.
23. Luo, Y.-D.; Dai, C.-A.; Chiu, W.-Y. *J. Polym. Sci., Part A: Polym. Chem.* **2008**, *46*, 1014.
24. Ugelstad, J.; Mórk, P. C.; Kaggerud, K. H.; Ellingsen, T.; Berge, A. *Adv. Colloid. Interface Sci.* **1980**, *13*, 101.
25. Zhou, X.; Ni, S.; Wang, X.; Wu, F. *Curr. Nanosci.* **2007**, *3*, 259.
26. Lan, Q.; Liu, C.; Yang, F.; Liu, S.; Xu, J.; Sun, D. *J. Colloid. Interface Sci.* **2007**, *310*, 260.
27. Corr, S. A.; Gun'ko, Y. K.; Tekoriute, R.; Meledandri, C. J.; Brougham, D. F. *J. Phys. Chem. C* **2008**, *112*, 13324.
28. Acar, H. Y.; Garaas, R. S.; Syud, F.; Bonitatebus, P.; Kulkarni, A. M. *J. Magn. Magn. Mater.* **2005**, *293*, 1.